Draft version October 15, 2026
Typeset using LaTeX **default** style in AASTeX7.0.1

First L-type substellar object discovered in the vicinity of the embedded cluster NGC 2023

Styliani Tsilia [1,2] Carlos Dominguez-Tagle [1,2] Maruša Žerjal [1,2] Eduardo L. Martín [1,2] Hervé Bouy [3,4] Nafise Sedighi [1,2] Sara Muñoz Torres [1,2] Nikola Vitas [1,2] Khalid Barkaoui [1,2,5,6] Nicolas Lodieu [1,2] and Jerry J.-Y. Zhang [7,8]

[1] *Instituto de Astrofísica de Canarias, Vía Láctea, 38205 La Laguna, Tenerife, Spain*
[2] *Universidad de La Laguna, Departamento de Astrofísica, 38206 La Laguna, Tenerife, Spain*
[3] *Laboratoire d'Astrophysique de Bordeaux, CNRS and Université de Bordeaux, Allée Geoffroy St. Hilaire, 33165 Pessac, France*
[4] *Institut universitaire de France (IUF), 1 rue Descartes, 75231 PARIS CEDEX 05, France*
[5] *Astrobiology Research Unit, Université de Liège, 19C Allée du 6 Août, 4000 Liège, Belgium*
[6] *Department of Earth, Atmospheric and Planetary Science, Massachusetts Institute of Technology, 77 Massachusetts Avenue, Cambridge, MA 02139, USA*
[7] *Department of Physics and Astronomy, The University of Western Ontario, 1151 Richmond St, London, ON N6A 3K7, Canada*
[8] *Institute for Earth and Space Exploration, The University of Western Ontario, 1151 Richmond St, London, ON N6A 3K7, Canada*

ABSTRACT

We present the first substellar object in a star-forming region spectroscopically confirmed with *Euclid*, namely J054158.70-021031.4. This young and faint source is located close to the embedded open cluster NGC 2023. It has a spectral type of L3, a reddening of $A_V = 3$ mag, proper motion consistent with the nearby cluster NGC 2024, and a magnitude of ~ 24.5 in the *Euclid* optical band. At the distance of 403 pc, its inferred mass lies close to the planetary-mass boundary. We discovered the object by searching for ultracool dwarf candidates in the *Euclid* Early Release Observations. The search was based on photometric criteria, followed by the analysis of slitless 2D spectro-images in order to distinguish features that indicate the nature of these objects. This work demonstrates the potential of *Euclid* to unveil previously hidden populations of very low-mass objects, located in obscured regions where star formation is ongoing.

Keywords: Stellar Astronomy (1583) — Star forming regions (1565) — Open star clusters (1160) — Free floating planets (549) — Brown dwarfs (185) — L dwarfs (894)

1. INTRODUCTION

Beyond the hydrogen-burning mass limit set at $\sim 0.08\,M_\odot$ (S. S. Kumar 1963; C. Hayashi & T. Nakano 1963), towards the very low-mass end of the mass spectrum, we encounter the regime of substellar objects. These sources include brown dwarfs and free-floating planetary-mass objects. Together with very low-mass stars they comprise the category of sources known as ultracool dwarfs (UCDs), which are objects of spectral type M7 and later (J. D. Kirkpatrick et al. 1997) corresponding to effective temperatures below ~ 2700 K (J. C. Filippazzo et al. 2015). UCDs are difficult to observe due to their intrinsic faintness, and many open questions persist about their exact formation mechanisms, their evolution and atmospheric properties.

Yet these objects are highly significant; acting as a bridge between stars and planets, they are numerous both in young open clusters and the field (K. Peña Ramírez et al. 2012; J. D. Kirkpatrick et al. 2021) and therefore essential to construct a complete picture of star formation processes. Their cool temperatures allow molecular species and grains of dust to survive in their atmospheres (J. D. Kirkpatrick 2005). Moreover, understanding how the initial mass function (IMF) extends into the very low-mass regime (e.g., J. D. Kirkpatrick et al. 2024), and how it might be influenced by environmental factors (e.g., M. R. Bate 2025), is crucial for connecting the core mass function (CMF) to the final outcome of star formation.

Email: stsilia@iac.es

Young star-forming regions provide a crucial laboratory for probing the very low-mass regime. UCDs keep fading over time, so young regions allow us to detect them at their brightest phase, reaching down to just a few Jupiter masses (e.g., K. Peña Ramírez et al. 2012). Unlike field populations, young regions offer access to samples of objects before dynamical evolution significantly modifies their spatial distribution. Hence these objects preserve information about their formation, and can provide good constrains on the IMF. Orion has been the target of numerous searches for very low-mass objects. Early work identified L-type members in σ Orionis already more than two decades ago (see, e.g., E. L. Martín et al. 2001). Subsequent surveys extended the substellar census across several Orion populations, including Orion OB1a and OB1b (J. J. Downes et al. 2008), the Trapezium Cluster (P. W. Lucas et al. 2005, 2006), NGC 2024 (J. L. Levine et al. 2006), σ Orionis (K. Peña Ramírez et al. 2012), and Barnard 30 (D. Barrado et al. 2026). In contrast, the local environment around NGC 2023 and the Horsehead Nebula remains underexplored at substellar masses. This relatively close (~ 400 pc) field is a star-forming region featuring a structure shaped by strong radiation fields and dense molecular material (E. Habart et al. 2005). The region lies at the interface between molecular gas and the radiation from nearby massive stars, making it a prime example of an environment influenced by stellar feedback processes such as photoionization and radiation-driven compression. The study of such regions can highlight the role of local cloud structure in shaping the lowest-mass products of star formation.

One powerful tool in the search for very low-mass objects is the *Euclid* space mission. It has already unveiled thousands of UCD candidates and hundreds of new spectroscopically confirmed UCDs (E. L. Martín et al. 2025; H. Bouy et al. 2025; M. Žerjal et al. 2025; C. Dominguez-Tagle et al. 2025; A. Mohandasan et al. 2025), demonstrating its sensitivity down to $\sim 4\,M_{Jup}$ at the distance of Orion (E. L. Martín et al. 2025), thanks to the performance of its Visible Camera (VIS; Euclid Collaboration et al. 2025a) and Near-Infrared Spectrometer and Photometer (NISP; Euclid Collaboration et al. 2025b). *Euclid's* VIS instrument provides high-resolution imaging in a single broad optical band (0.55–0.90 µm, hereafter referred to as I_E) with an angular resolution of $\sim 0\farcs1$. The second instrument, NISP, operates in the near-infrared, providing images in the Y_E (0.92–1.14 µm), J_E (1.14–1.37 µm), and H_E (1.37–2.00 µm) photometric bands, and slitless spectroscopy over 1.1–2.0 µm with a resolving power $R \approx 450$. *Euclid's* Wide Survey is able to detect sources down to nominal survey completeness limits of 24.5 mag in the NISP bands (AB, 5σ point-source depth) and 26.2 mag in the VIS band (Euclid Collaboration et al. 2022). *Euclid's* Deep Survey is expected to reach 2 magnitudes deeper (Euclid Collaboration et al. 2021). *Euclid* delivers a wide field of view (FoV) per pointing, with footprints of $\sim 0.54\,deg^2$ for VIS (Euclid Collaboration et al. 2025a) and $\sim 0.57\,deg^2$ for NISP (Euclid Collaboration et al. 2025b).

In this work, we exploit for the first time *Euclid* observations to successfully identify an L3-type substellar object in an embedded region, where both reddening and negligible proper motions limit conventional searches. We take the first step towards probing the substellar population of this challenging environment, pushing the low-mass limit of the known population towards the planetary-mass regime.

2. DATA

This paper utilizes the *Euclid* Early Release Observations (ERO) program. More specifically it focuses on the Barnard 33 (Horsehead Nebula) field, one of the pointings included in project ERO-02[9] (P.I. Eduardo Martín) which targeted nearby star-forming regions (distance ≤ 400 pc) and very young open clusters (age ≤ 10 Myr).

In this work we used photometric data from *Euclid*, processed by the pipeline of J.-C. Cuillandre et al. (2025), as well as a denebulized photometric catalog. The denebulized catalog was constructed by applying a novel deep learning algorithm (DeNeb; Bertin et al., in prep.) able to distinguish between the nebula and point source components in the images (for a more detailed description of this algorithm, see A. R. G. do Brito do Vale et al. 2026). We complemented *Euclid* data with ancillary observations from the *Spitzer* mission (M. W. Werner et al. 2004) in the IRAC [3.6] and [4.5] channels with central wavelengths of 3.56 µm and 4.52 µm respectively (G. G. Fazio et al. 2004), which we processed with DeNeb as well. Denebulized data is explicitly noted in the plots by using DeNeb's name next to the name of each denebulized band.

3. CANDIDATE SELECTION AND CONFIRMATION

Our search focused only on the high-reddening region of the *Euclid* ERO Barnard 33 field; the low-reddening area has been studied by E. L. Martín et al. (2025) and Dominguez-Tagle et al. (in prep.). We set a constant right ascension

[9] https://euclid.esac.esa.int/dr/ero/

(RA) value of 85.18750°as the boundary between these two regions. We filtered the denebulized photometric catalog, requiring a signal-to-noise ratio (S/N) ≥ 3 in the J_E band (where we expect substellar objects to be the brightest). This selection cut was kept minimal and did not include morphological criteria, to ensure we would not accidentally filter out true members of the star-forming region. Subsequently we constructed a grid of color-magnitude diagrams (CMDs) combining data from *Euclid* with *Spitzer*, including only objects with valid photometry in each individual plot, and overlaying ATMO isochrones (M. W. Phillips et al. 2020) for 1 to 7 Myr, consistent with the range of ages reported in the literature for this region (see M. A. López-García et al. 2013, and references therein). The models were converted from the Vega to the AB photometric system and calculated for a distance of 403±5 pc. This distance was based on the value that S. A. Dzib et al. (2026) calculated for NGC 2024 and was considered as the most reliable proxy since NGC 2023 and NGC 2024 are part of the same cluster grouping within the Orion B molecular cloud. As reddening might shift the colors of sources towards the red part of the CMDs, coeval objects did not necessary lie along the same isochrone. Therefore, in order to compile a list of preliminary candidates, we counted every object consistently redder than an isochrone in every CMD where the object appeared. We repeated this for every isochrone, also retaining sources lying up to 0.25 mag blueward of each isochrone to account for uncertainties. This margin was based on the CMD position of the benchmark objects listed in E. L. Martín et al. (2025). This process yielded a preliminary list of 3148 candidates.

Given the particularities of this field (i.e., nebulae, reddening and artifacts), we filtered out the list of candidates to accelerate the selection, by reviewing the NISP slitless 2D spectro-images. In the wavelength range of NISP, the spectra of substellar objects show characteristic strong absorption bands of H_2O. This feature translates into a drop in brightness that is evident even in the 2D spectro-images. The list of candidates for spectra extraction was limited to ~ 20.5 mag in the J_E band, in order to obtain spectra where the depth of H_2O absorption bands had a S/N > 10, as described in Dominguez-Tagle et al. (in prep.). We produced image cutouts for each object and carried out a visual inspection of the spectral traces. We selected those that clearly exhibited substellar-like features in order to be extracted. The details of this method of candidate selection and prioritization through visual examination are included in Tsilia et al. (in prep.), which describes the full analysis of all the objects in this field. Even though this visual technique could include some bias, it has allowed us to go through the artifacts and contamination present in slitless spectroscopy. It has also been very useful in a highly populated region with the presence of nebulae. It has allowed us to confirm or reject the UCD nature of candidates, given the available data in the most efficient way possible.

In the process of reviewing the candidates, the first we found to showcase the characteristic UCD spectral features was at coordinates J054158.70-021031.4. Hereafter, we refer to the source as J0541 for brevity. We then extracted the 1D spectrum. As described in Euclid Collaboration et al. (2022), *Euclid* observations include four spectra by performing a dithering pattern. However, given that NISP has a mosaic of 16 detectors with gaps between them, all or part of the object spectrum could fall into these gaps for some of these dithering positions. In consequence, for a given object, the available spectra could go from zero to four. In the case of J0541, only one dithering position was available. We extracted the 1D spectrum using the collection of programs described in Dominguez-Tagle et al. (in prep.), which included the trace identification, the elimination of bad pixels, the subtraction of background and a box-car extraction aperture. We did the wavelength calibration using the cut-on and cut-off wavelengths of the red grism and fitting to the spectral dispersion measured by Euclid Collaboration et al. (2026). We corrected the instrumental response by the sensitivity curve of the spectrophotometric standard star GRW70 observed in the same NISP configuration as that of J0541. These first order calibrations were accurate enough to proceed with the classification by spectral type (SpT). We dereddened the spectrum for a range of A_V values from 0 to 10 mag with a step of 0.5 mag, using the J. A. Cardelli et al. (1989) extinction law. We compared all these dereddened spectra (smoothed with a boxcar = 3) to SpeX low-gravity standard templates (A. J. Burgasser 2014; A. J. Burgasser & Splat Development Team 2017) by χ^2 minimisation. The result is shown in the left panel of Fig. 1. The plot shows the χ^2 values for the comparison with all spectral types and extinction values. The minimum value is found for an $A_V = 3$ mag and the L3γ template (2MASSW J2208136+292121, J. Gagné et al. 2015). For the other standard templates, the minimum, although higher than that for L3γ, shifts to lower A_V values for later types and to higher ones for earlier types. We did the same comparison with field standard templates from the same catalogs, obtaining 3 times larger values for χ^2, which confirmed that the best fit corresponds to low-gravity standard templates. We computed the H-cont index defined by K. N. Allers & M. C. Liu (2013) to verify the triangular-shape of the H-band peak, which is representative of young objects. For the original spectrum, the H-cont index is 1.091 ± 0.077, and for the spectrum dereddened for $A_V = 3$ mag the H-cont index is 1.080 ± 0.071, which confirms the triangular shape. The right panel of Fig. 1 shows J0541 spectrum dereddened for

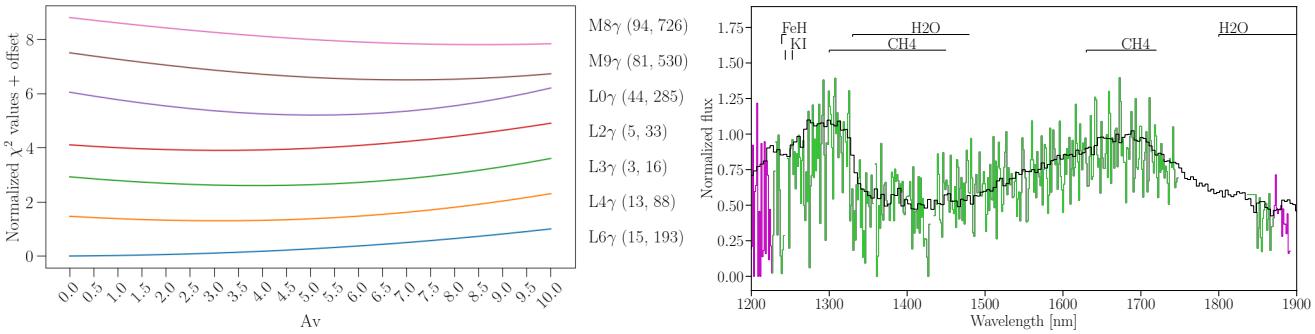


Figure 1. *Left:* χ^2 values for the comparison of the smoothed J0541 *Euclid* spectrum with young templates at different A_V values. The χ^2 values are normalized between each template minimum and maximum, which are written next to the template spectral type. *Right:* The *Euclid* spectrum of J0541 dereddened for $A_V = 3$ mag compared to an L3γ template. The spectrum is plotted by green and magenta lines, the latter corresponding to wavelengths of low grism transmission. No line is plotted where the spectrum is contaminated by artifacts. The L3γ template (2MASSW J2208136+292121, J. Gagné et al. 2015) is plotted by the black line.

$A_V = 3$ mag, compared to the L3γ template. Owing the contamination from artifacts, the flux for some wavelength values is masked. This spectrum confirms the candidate as a young L3 UCD.

4. THE NEW OBJECT

The newly discovered substellar object exhibits very low brightness, being almost as faint as 24.5 mag in the optical band, but becoming brighter as we move further into the infrared regime. A comparison of its photometry between the ERO pipeline and the denebulized catalog reveals that DeNeb primarily affected the Y_E-band photometry, resulting in redder $I_E - Y_E$, $Y_E - J_E$ and $Y_E - H_E$ colors by ~ 0.4 mag. This suggests that the deep learning algorithm successfully removed the contamination caused by nebulosity. The I_E, J_E and H_E measurements remain essentially the same. This comparison is seen in Table 1, where additional photometric measurements for this object from UKIDSS DR9 (A. Lawrence et al. 2007), the Spitzer Legacy catalog SESNA (R. Gutermuth et al. 2019), and VISTA/VIRCAM (the Science Verification Galactic mini-survey of Orion: M. Arnaboldi et al. 2010; M. Petr-Gotzens et al. 2011, as processed by A. Rottensteiner et al. 2026) are combined.

Using VOSA (A. Bayo et al. 2008) we inspected the spectral energy distribution (SED) curve for J0541 by combining the measurements exhibiting the lowest uncertainty: *Euclid's* denebulized photometry, data from VISTA Ks, and data from IRAC [3.6] and [4.5]. No obvious infrared excess was detected up to IRAC [4.5]. We also fitted ATMO 2020 CEQ (M. W. Phillips et al. 2020) models to the SED. For the gravity and effective temperature of the object, the best-fitting parameters were $\log g = 2.50$, $T_{\rm eff} = 1500$ K; the corresponding posterior 96% credible limits were 2.50-2.95 and 1400-1770 K, respectively. This temperature estimate is consistent, within its posterior 96% credible interval, with the expected temperature of an L3-type, low-gravity object (J. C. Filippazzo et al. 2015).

Additionally we checked narrow-band Brγ observations that we had obtained with the PANIC wide field near infrared camera at the Calar Alto 2.2 m telescope (M.-C. Cárdenas Vázquez et al. 2018) on 3 nights between 6-8 December 2025 (P.I. Sara Muñoz Torres). J0541 does not show obvious excess in the emission line. These observations will be further analyzed in future work.

J0541 is located approximately 7.5 arcmin away from the center of NGC 2023, which translates to ~ 0.9 pc away from the cluster center at the distance of the cluster. An image cutout is given in the left panel of Fig. 2, where the object clearly appears as a point source. This region has been studied before, and several sources have been discovered in the same FoV. We note the presence of young stellar objects (YSOs) (see Gaia Collaboration et al. 2021; S. T. Megeath et al. 2012; R. M. Cutri et al. 2003; B. Mookerjea et al. 2009), typical of a region undergoing star formation, and also the abundance of dense cores that seem almost evenly spread out (see V. Könyves et al. 2020; S. Dutta et al. 2020; H. Kirk et al. 2016; B. Mookerjea et al. 2009). Their spatial distribution is plotted in the right panel of Fig. 2. B. Mookerjea et al. (2009) suggest that the expansion of the IC 434 HII region (located just south of the Horsehead Nebula) compresses gas in dense, pillar-like structures, triggering star formation in this region.

Now we examine J0541 relative to the new UCD candidates and previously known objects that E. L. Martín et al. (2025) reported in the low-reddening region of the *Euclid* ERO Barnard 33 field. Additionally, we plot the same sources in color-color diagrams. An indicative CMD is shown in the left panel of Fig. 3. As mentioned in Section 3,

Table 1. Photometric measurements for J0541.

Band	ERO pipeline	DeNeb	UKIDSS	VISTA	IRAC
I_E	24.46±0.04	24.48±0.05	—	—	—
Y_E	20.79±0.002	20.38±0.02	—	—	—
J_E	19.48±0.001	19.48±0.01	—	—	—
H_E	18.82±0.001	18.77±0.01	—	—	—
Y	—	—	20.06±0.21	—	—
J	—	—	18.58±0.10	18.56±0.02	
H	—	—	17.4±0.06	17.35±0.02	—
K	—	—	16.47±0.05	—	—
Ks	—	—	—	16.48±0.02	—
[3.6]	—	—	—	—	15.58±0.04
[4.5]	—	—	—	—	15.43±0.05
[5.8]	—	—	—	—	15.72±0.50

Note—All values are in magnitudes. *Euclid's* bands are given in the AB system, all other bands in the Vega system. Whenever multiple data points are available for the same band, the measurement with the smallest uncertainty is displayed.

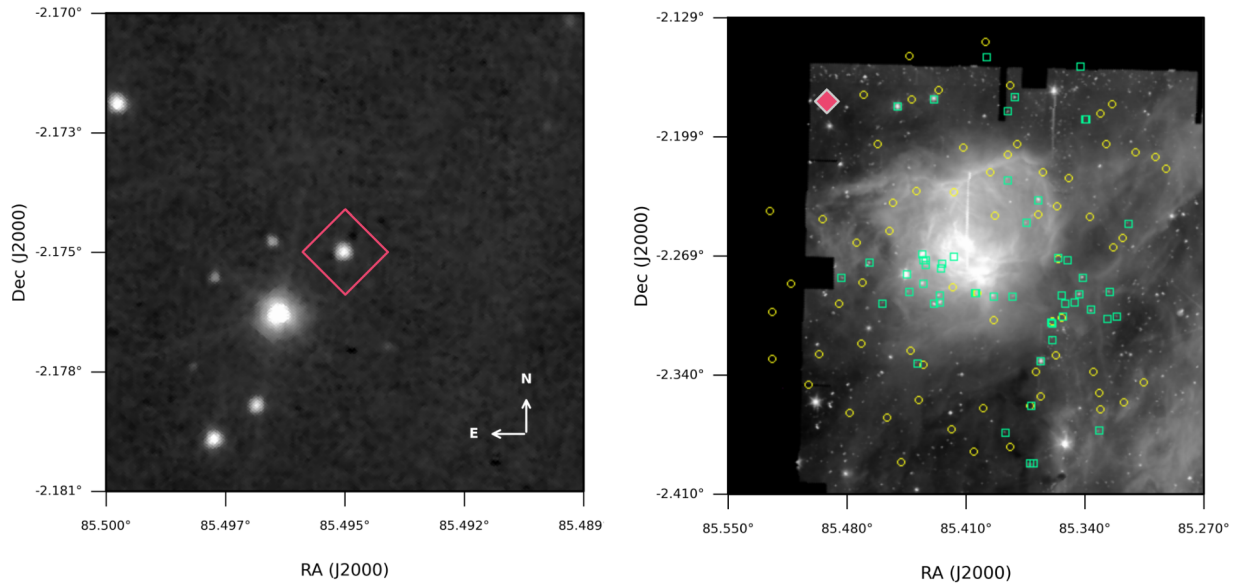


Figure 2. *Left: Euclid* J_E cutout centered on the source of interest (J054158.70-021031.4). *Right:* Spatial distribution of YSOs (denoted as green squares) and dense cores (denoted as yellow circles) falling within 8 arcmin from NGC 2023. J0541 is marked as a pink rhomb in both plots.

our full candidate selection considered isochrones spanning 1–7 Myr, but here we show the 1 and 3 Myr isochrones as representative models for the young population. The selection of J0541 is insensitive to the adopted age within the 1–7 Myr range. J0541 is well separated to the right of the models, which is expected for a reddened object, and is almost as faint as the faintest sources detected in E. L. Martín et al. (2025). We dereddened it using the value of $A_V = 3$ mag that we found above, and the J. A. Cardelli et al. (1989) extinction law. The dereddened source is in good agreement with the sequence of the rest of the objects. The plot also reveals that J0541 is located close to the deuterium-burning mass limit of $\sim 13\,M_{Jup}$ (D. S. Spiegel et al. 2011), and could be of planetary mass, depending on

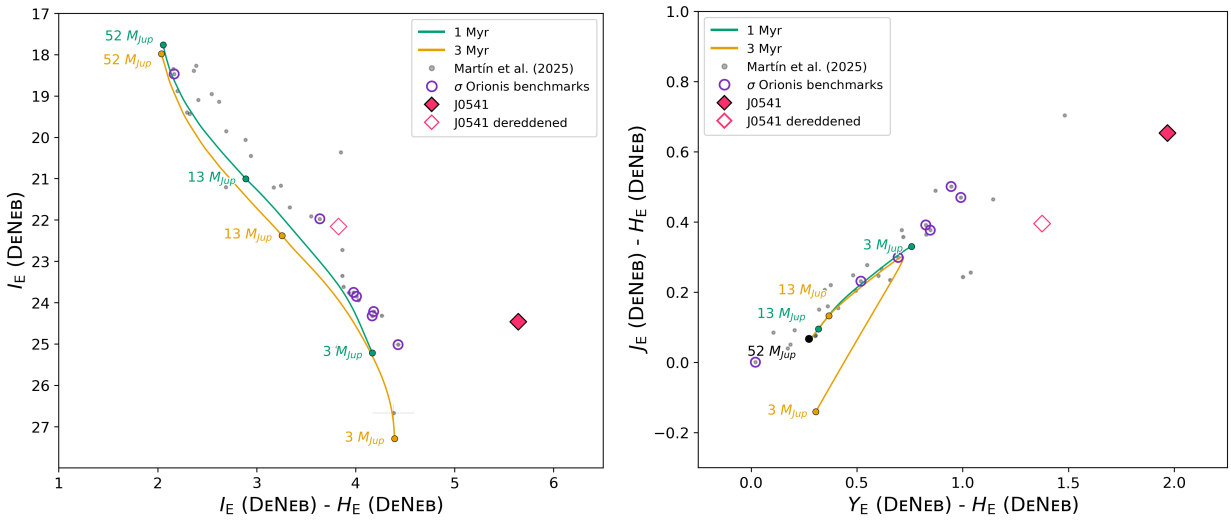


Figure 3. Plots showing J0541 compared to the new UCD candidates and previously known objects listed in E. L. Martín et al. (2025). J0541 is marked as a pink rhomb, benchmark objects are marked as purple circles, and the ATMO CEQ isochrones (see M. W. Phillips et al. 2020) for the ages of 1 and 3 Myr and a distance of 403 pc are drawn. J0541 is also shown dereddened using $A_V = 3$ mag and $R_V = 3.1$. *Left:* CMD of I_E versus I_E-H_E. *Right:* Color-color diagram of J_E-H_E versus Y_E-H_E. The 52 M_{Jup} point overlaps for the two isochrones.

its exact age. An indicative color-color diagram is shown in the right panel of Fig. 3. Once again we dereddened J0541 using $A_V = 3$ mag. We note that it lies further away from most of the other sources with respect to the isochrones, but we caution that the theoretical isochrones do not accurately reproduce the observed colors and are shown only as a qualitative reference.

As an empirical assessment of the mass–extinction range accessible at the depth demonstrated by J0541, we used the 1 and 3 Myr isochrones at 403 pc to calculate the extinction required for objects of different masses to reach the observed $I_E = 24.46$ mag. Objects of ∼8, 13, 30 and 51 M_{Jup} reach this reference magnitude at $A_V \simeq 0.9$–3.0, 2.7–4.5, 6.8–7.3 and 8.4–8.7 mag respectively, while a 3 Myr and ∼5 M_{Jup} model is already fainter without extinction. Thus, at the depth of J0541, sensitivity to extinction increases strongly with mass and decreases with age at the lowest masses.

The proper motion of this object was found by A. Rottensteiner et al. (2026) to be $\simeq 1.19 \pm 0.35$ mas yr^{-1} in RA and $\simeq -1.97 \pm 0.21$ mas yr^{-1} in Dec, based on multi-epoch infrared observations carried out with the VISTA/VIRCAM instrument through three different surveys: the Science Verification Galactic mini-survey of Orion (M. Arnaboldi et al. 2010; M. Petr-Gotzens et al. 2011), the Vista Hemisphere Survey (R. G. McMahon et al. 2013), and the VISIONS survey (S. Meingast et al. 2023). The left panel of Fig. 4 shows the direction of this motion (away from NGC 2024 on the plane of the sky), alongside the proper motions of the confirmed YSOs considered by A. Rottensteiner et al. (2026) as NGC 2024 members, and also the proper motions (wherever available) of any additional YSOs located within 8 arcmin from NGC 2023. The proper motion of J0541 is low, consistent with the Orion star-forming complex, its youth also suggesting that it is not found far away from its birthplace. It is not included in the list of NGC 2024 members from A. Rottensteiner et al. (2026), but in proper-motion space, J0541 falls inside the 1σ covariance ellipse defined by those members (right panel of Fig. 4). The Mahalanobis distance between J0541 and the cluster centroid is $D = 0.48$, suggesting a high degree of kinematic similarity to the NGC 2024 population, and supporting J0541 as a possible outer member of the cluster. The proper motions of YSOs located within 8 arcmin of NGC 2023 are shown for comparison, but their membership status is yet to be assessed. No proper-motion study of NGC 2023 is currently available, highlighting the need for such an investigation.

5. SUMMARY

In this work we searched for substellar objects in a region of intermediate and spatially variable reddening. We combined ERO data from *Euclid* (broad-band photometry and spectroscopy) with archival observations from *Spitzer* (broad-band photometry). We applied photometric criteria to compile a list of candidates, then we visually inspected their spectral traces to identify objects that exhibited substellar characteristics. We present a new spectroscopically confirmed substellar object of spectral type L3 and reddening $A_V = 3$ mag, the first object of such late spectral type

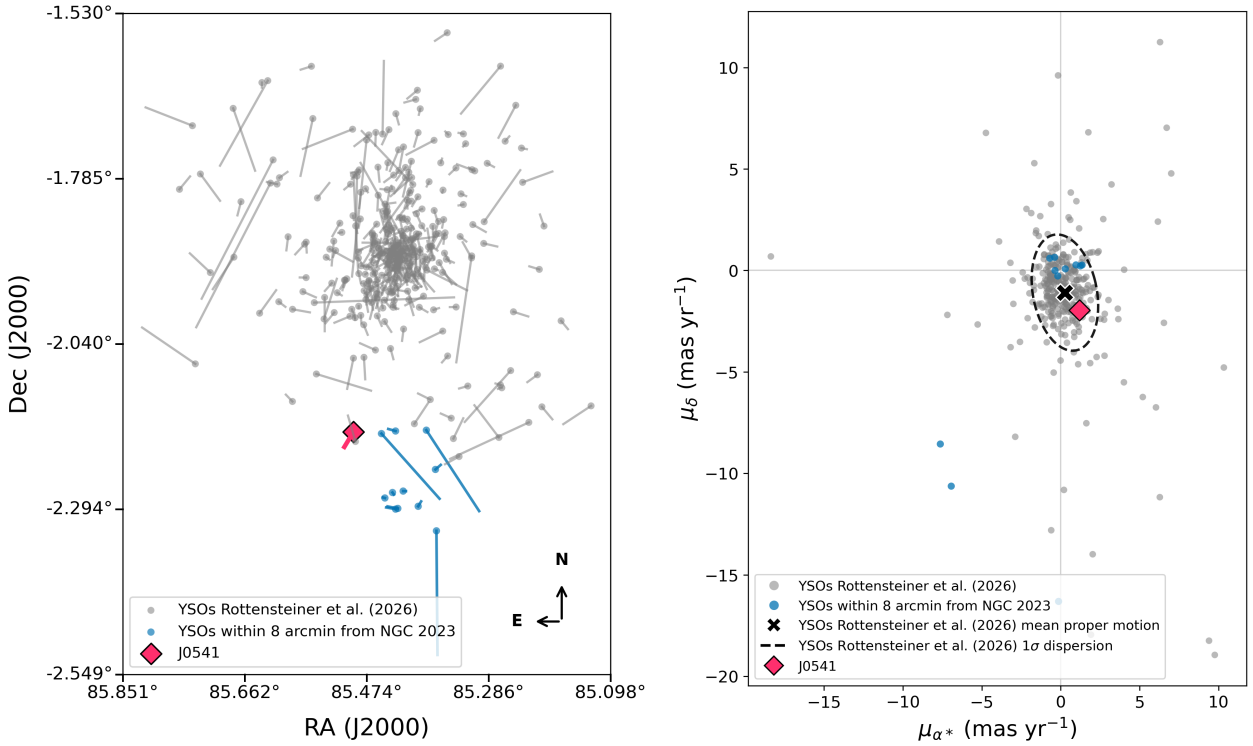


Figure 4. Proper motion of J0541 (marked as a pink rhomb) compared to proper motions of YSOs in the nearby environment. Members of NGC 2024 are denoted in gray, while additional objects within 8 arcmin from the center of NGC 2023 are denoted in blue. Only proper motions with S/N $\geq$ 3 are plotted. *Left:* The spatial distribution of sources is shown together with the direction of their proper motion. Velocities are shown in arbitrary units. *Right:* Proper motion diagram. The black cross marks the mean proper motion of the cluster's members. The black dashed line denotes the 1σ covariance ellipse. The proper motion error for J0541 is smaller than the symbol.

to be discovered in this embedded area. This source lies close to the deuterium-burning mass limit, and could be of planetary mass, depending on its exact age.

The membership of J0541 in the Orion star-forming complex is supported by its location on the plane of the sky in proximity to NGC 2023 ($\sim$ 7.5 arcmin) and NGC 2024 ($\sim$ 20 arcmin), its near-infrared spectrum indicative of youth, its position in the CMDs in good agreement with theoretical isochrones, and its proper motion which is consistent with the NGC 2024 population. Its interstellar extinction further argues against an unreddened foreground origin.

Multiple YSOs and dense cores have been discovered around NGC 2023. This star-forming region serves as a potential laboratory for investigating how stellar feedback and local cloud structure shape the products of star formation. Now for the first time we are able to probe the substellar population of this dynamic environment, with J0541 effectively pushing the low-mass limit of the population in this region.

Objects of spectral type L3 or later have been identified in star-forming regions before (e.g., C. Alves de Oliveira et al. 2012). However, young ultracool populations in star-forming environments affected by spatially variable extinction remain challenging to identify and characterize over large areas. J0541 is simultaneously of spectral type L3, young, close to the planetary-mass boundary, and affected by intermediate reddening. This combination makes it a useful example of a young L-type object still associated with its natal cloud environment.

Our discovery highlights *Euclid's* ability to reveal young substellar objects in moderately obscured star-forming environments. J0541 therefore becomes a reference for the study of embedded very low-mass populations with wide-field, space-based surveys such as *Euclid* and the upcoming *Nancy Grace Roman Space Telescope*. Such wide-field surveys are also highly complementary to the *James Webb Space Telescope* (JWST); while JWST can probe deeply embedded populations at high extinction, *Euclid* can extend searches for young, very low-mass objects over much larger areas at lower extinction. J0541 thus represents a compelling target for JWST follow-up, illustrating the potential synergy between wide-field discovery with *Euclid* and detailed characterization with JWST.

ACKNOWLEDGMENTS

We thank I. Baraffe and M. Phillips for making available a digitized version of their ATMO isochrones in the *Euclid* passbands. Funding for ST, MŽ, CDT, ELM, NS, SMT, NV, KB and JYZ was provided by the European Union (ERC Advanced Grant, SUBSTELLAR, project number 101054354). NL acknowledges support from the Agencia Estatal de Investigación del Ministerio de Ciencia e Innovación (AEI-MCINN) under grant PID2022-137241NB-C41. JYZ thanks the support from the Western Postdoctoral Fellowship provided by Western University. This work is part of grant CEX2025-001609-S, awarded to the Instituto de Astrofísica de Canarias under the Severo Ochoa Centre of Excellence program and funded by MICIU/AEI/10.13039/501100011033. This work has made use of the Early Release Observations (ERO) data from the *Euclid* mission of the European Space Agency (ESA), 2024, https://doi.org/10.57780/esa-qmocze3. The authors acknowledge the *Euclid* Consortium, the European Space Agency, and a number of agencies and institutes that have supported the development of *Euclid*, in particular the Agenzia Spaziale Italiana, the Austrian Forschungsfüörderungsgesellschaft funded through BMK, the Belgian Science Policy, the Canadian *Euclid* Consortium, the Deutsches Zentrum für Luft- und Raumfahrt, the DTU Space and the Niels Bohr Institute in Denmark, the French Centre National d'Etudes Spatiales, the Fundação para a Ciência e a Tecnologia, the Hungarian Academy of Sciences, the Ministerio de Ciencia, Innovación y Universidades, the National Aeronautics and Space Administration, the National Astronomical Observatory of Japan, the Netherlandse Onderzoekschool Voor Astronomie, the Norwegian Space Agency, the Research Council of Finland, the Romanian Space Agency, the State Secretariat for Education, Research, and Innovation (SERI) at the Swiss Space Office (SSO), and the United Kingdom Space Agency. A complete and detailed list is available on the *Euclid* web site (www.euclid-ec.org). This work is based in part on observations made with the *Spitzer* Space Telescope, which was operated by the Jet Propulsion Laboratory, California Institute of Technology under a contract with NASA. This work is based in part on observations collected at the Centro Astronómico Hispano en Andalucía (CAHA) at Calar Alto, proposal 25B-2.2-023, operated jointly by Junta de Andalucía and Consejo Superior de Investigaciones Científicas (IAA-CSIC). This work is based in part on data obtained as part of the UKIDSS project, defined in A. Lawrence et al. (2007). UKIDSS uses the UKIRT Wide Field Camera (WFCAM; M. Casali et al. 2007). The photometric system is described in P. C. Hewett et al. (2006), and the calibration is described in (S. T. Hodgkin et al. 2009). The pipeline processing and science archive are described in Irwin et al. (in prep.) and N. C. Hambly et al. (2008). This work is based in part on observations made with VISTA (J. Emerson et al. 2006; G. B. Dalton et al. 2006). This research has made use of the SIMBAD database (M. Wenger et al. 2000) operated at CDS, Strasbourg, France, and of the Astrophysics Data System, funded by NASA under Cooperative Agreement 80NSSC21M0056. This research has made use of the VizieR catalogue access tool, CDS, Strasbourg, France (F. Ochsenbein 1996). The original description of the VizieR service was published in F. Ochsenbein et al. (2000) This research has made use of "Aladin sky atlas" (F. Bonnarel et al. 2000) developed at CDS, Strasbourg Observatory, France. This publication makes use of VOSA (A. Bayo et al. 2008), developed under the Spanish Virtual Observatory (https://svo.cab.inta-csic.es) project funded by MCIN/AEI/10.13039/501100011033 through grant PID2023-146210NB-I00. VOSA has been partially updated by using funding from the European Union's Horizon 2020 Research and Innovation Programme, under Grant Agreement nº 776403 (EXOPLANETS-A). This research has made use of the SVO Filter Profile Service "Carlos Rodrigo" (C. Rodrigo & E. Solano 2020; C. Rodrigo et al. 2012), funded by MCIN/AEI/10.13039/501100011033/ through grant PID2023-146210NB-I00. Software: `astropy` (Astropy Collaboration et al. 2018), `NumPy` (C. R. Harris et al. 2020), `matplotlib` (J. D. Hunter 2007), `IPython` (F. Perez & B. E. Granger 2007), and `TOPCAT` (M. B. Taylor 2005).

REFERENCES

Allers, K. N., & Liu, M. C. 2013, ApJ, 772, 79, doi: 10.1088/0004-637X/772/2/79

Alves de Oliveira, C., Moraux, E., Bouvier, J., & Bouy, H. 2012, A&A, 539, A151, doi: 10.1051/0004-6361/201118230

Arnaboldi, M., Petr-Gotzens, M., Rejkuba, M., et al. 2010, The Messenger, 139, 6

Astropy Collaboration, Price-Whelan, A. M., Sipőcz, B. M., et al. 2018, AJ, 156, 123, doi: 10.3847/1538-3881/aabc4f

Barrado, D., Bouy, H., Martin, E. L., et al. 2026, arXiv e-prints, arXiv:2608.07048, doi: 10.48550/arXiv.2608.07048

Bate, M. R. 2025, MNRAS, 537, 752, doi: 10.1093/mnras/staf059

Bayo, A., Rodrigo, C., Barrado Y Navascués, D., et al. 2008, A&A, 492, 277, doi: 10.1051/0004-6361:200810395
Bonnarel, F., Fernique, P., Bienaymé, O., et al. 2000, A&AS, 143, 33, doi: 10.1051/aas:2000331
Bouy, H., Martín, E. L., Cuillandre, J.-C., et al. 2025, A&A, 696, A80, doi: 10.1051/0004-6361/202553979
Burgasser, A. J. 2014, in Astronomical Society of India Conference Series, Vol. 11, Astronomical Society of India Conference Series, 7–16, doi: 10.48550/arXiv.1406.4887
Burgasser, A. J., & Splat Development Team. 2017, in Astronomical Society of India Conference Series, Vol. 14, Astronomical Society of India Conference Series, 7–12, doi: 10.48550/arXiv.1707.00062
Cardelli, J. A., Clayton, G. C., & Mathis, J. S. 1989, ApJ, 345, 245, doi: 10.1086/167900
Cárdenas Vázquez, M.-C., Dorner, B., Huber, A., et al. 2018, PASP, 130, 025003, doi: 10.1088/1538-3873/aa9884
Casali, M., Adamson, A., Alves de Oliveira, C., et al. 2007, A&A, 467, 777, doi: 10.1051/0004-6361:20066514
Cuillandre, J.-C., Bertin, E., Bolzonella, M., et al. 2025, A&A, 697, A6, doi: 10.1051/0004-6361/202450803
Cutri, R. M., Skrutskie, M. F., van Dyk, S., et al. 2003, VizieR Online Data Catalog: 2MASS All-Sky Catalog of Point Sources (Cutri+ 2003),, VizieR On-line Data Catalog: II/246. Originally published in: University of Massachusetts and Infrared Processing and Analysis Center, (IPAC/California Institute of Technology) (2003)
Dalton, G. B., Caldwell, M., Ward, A. K., et al. 2006, in Society of Photo-Optical Instrumentation Engineers (SPIE) Conference Series, Vol. 6269, Ground-based and Airborne Instrumentation for Astronomy, ed. I. S. McLean & M. Iye, 62690X, doi: 10.1117/12.670018
do Brito do Vale, A. R. G., Mužić, K., Bouy, H., et al. 2026, A&A, 706, A149, doi: 10.1051/0004-6361/202557493
Dominguez-Tagle, C., Žerjal, M., Sedighi, N., et al. 2025, ApJ, 991, 84, doi: 10.3847/1538-4357/adf72d
Downes, J. J., Briceño, C., Hernández, J., et al. 2008, AJ, 136, 51, doi: 10.1088/0004-6256/136/1/51
Dutta, S., Lee, C.-F., Liu, T., et al. 2020, ApJS, 251, 20, doi: 10.3847/1538-4365/abba26
Dzib, S. A., Ordóñez-Toro, J., Loinard, L., et al. 2026, A&A, 708, A299, doi: 10.1051/0004-6361/202558169
Emerson, J., McPherson, A., & Sutherland, W. 2006, The Messenger, 126, 41
Euclid Collaboration, Pocino, A., Tutusaus, I., et al. 2021, A&A, 655, A44, doi: 10.1051/0004-6361/202141061
Euclid Collaboration, Scaramella, R., Amiaux, J., et al. 2022, A&A, 662, A112, doi: 10.1051/0004-6361/202141938
Euclid Collaboration, Cropper, M. S., Al-Bahlawan, A., et al. 2025a, A&A, 697, A2, doi: 10.1051/0004-6361/202450996
Euclid Collaboration, Jahnke, K., Gillard, W., et al. 2025b, A&A, 697, A3, doi: 10.1051/0004-6361/202450786
Euclid Collaboration, Gillard, W., Maciaszek, T., et al. 2026, A&A, 707, A227, doi: 10.1051/0004-6361/202555859
Fazio, G. G., Hora, J. L., Allen, L. E., et al. 2004, ApJS, 154, 10, doi: 10.1086/422843
Filippazzo, J. C., Rice, E. L., Faherty, J., et al. 2015, ApJ, 810, 158, doi: 10.1088/0004-637X/810/2/158
Gagné, J., Faherty, J. K., Cruz, K. L., et al. 2015, ApJS, 219, 33, doi: 10.1088/0067-0049/219/2/33
Gaia Collaboration, Brown, A. G. A., Vallenari, A., et al. 2021, A&A, 649, A1, doi: 10.1051/0004-6361/202039657
Gutermuth, R., Dunham, M., & Offner, S. 2019, in American Astronomical Society Meeting Abstracts, Vol. 233, American Astronomical Society Meeting Abstracts #233, 367.10
Habart, E., Abergel, A., Walmsley, C. M., Teyssier, D., & Pety, J. 2005, A&A, 437, 177, doi: 10.1051/0004-6361:20041546
Hambly, N. C., Collins, R. S., Cross, N. J. G., et al. 2008, MNRAS, 384, 637, doi: 10.1111/j.1365-2966.2007.12700.x
Harris, C. R., Millman, K. J., van der Walt, S. J., et al. 2020, Nature, 585, 357, doi: 10.1038/s41586-020-2649-2
Hayashi, C., & Nakano, T. 1963, Progress of Theoretical Physics, 30, 460, doi: 10.1143/PTP.30.460
Hewett, P. C., Warren, S. J., Leggett, S. K., & Hodgkin, S. T. 2006, MNRAS, 367, 454, doi: 10.1111/j.1365-2966.2005.09969.x
Hodgkin, S. T., Irwin, M. J., Hewett, P. C., & Warren, S. J. 2009, MNRAS, 394, 675, doi: 10.1111/j.1365-2966.2008.14387.x
Hunter, J. D. 2007, Computing in Science and Engineering, 9, 90, doi: 10.1109/MCSE.2007.55
Kirk, H., Di Francesco, J., Johnstone, D., et al. 2016, ApJ, 817, 167, doi: 10.3847/0004-637X/817/2/167
Kirkpatrick, J. D. 2005, ARA&A, 43, 195, doi: 10.1146/annurev.astro.42.053102.134017
Kirkpatrick, J. D., Henry, T. J., & Irwin, M. J. 1997, AJ, 113, 1421, doi: 10.1086/118357
Kirkpatrick, J. D., Gelino, C. R., Faherty, J. K., et al. 2021, ApJS, 253, 7, doi: 10.3847/1538-4365/abd107
Kirkpatrick, J. D., Marocco, F., Gelino, C. R., et al. 2024, ApJS, 271, 55, doi: 10.3847/1538-4365/ad24e2
Könyves, V., André, P., Arzoumanian, D., et al. 2020, A&A, 635, A34, doi: 10.1051/0004-6361/201834753
Kumar, S. S. 1963, ApJ, 137, 1121, doi: 10.1086/147589

Lawrence, A., Warren, S. J., Almaini, O., et al. 2007, MNRAS, 379, 1599, doi: 10.1111/j.1365-2966.2007.12040.x

Levine, J. L., Steinhauer, A., Elston, R. J., & Lada, E. A. 2006, ApJ, 646, 1215, doi: 10.1086/504964

López-García, M. A., López-Santiago, J., Albacete-Colombo, J. F., Pérez-González, P. G., & de Castro, E. 2013, MNRAS, 429, 775, doi: 10.1093/mnras/sts373

Lucas, P. W., Roche, P. F., & Tamura, M. 2005, MNRAS, 361, 211, doi: 10.1111/j.1365-2966.2005.09156.x

Lucas, P. W., Weights, D. J., Roche, P. F., & Riddick, F. C. 2006, MNRAS, 373, L60, doi: 10.1111/j.1745-3933.2006.00244.x

Martín, E. L., Zapatero Osorio, M. R., Barrado y Navascués, D., Béjar, V. J. S., & Rebolo, R. 2001, ApJL, 558, L117, doi: 10.1086/323633

Martín, E. L., Žerjal, M., Bouy, H., et al. 2025, A&A, 697, A7, doi: 10.1051/0004-6361/202450793

McMahon, R. G., Banerji, M., Gonzalez, E., et al. 2013, The Messenger, 154, 35

Megeath, S. T., Gutermuth, R., Muzerolle, J., et al. 2012, AJ, 144, 192, doi: 10.1088/0004-6256/144/6/192

Meingast, S., Alves, J., Bouy, H., et al. 2023, A&A, 673, A58, doi: 10.1051/0004-6361/202245771

Mohandasan, A., Smart, R. L., Reyl\'e, C., et al. 2025, arXiv e-prints, arXiv:2503.22559, doi: 10.48550/arXiv.2503.22559

Mookerjea, B., Sandell, G., Jarrett, T. H., & McMullin, J. P. 2009, A&A, 507, 1485, doi: 10.1051/0004-6361/200912550

Ochsenbein, F. 1996, The VizieR database of astronomical catalogues, CDS, Centre de DonnÃ©es astronomiques de Strasbourg, doi: 10.26093/CDS/VIZIER

Ochsenbein, F., Bauer, P., & Marcout, J. 2000, A&AS, 143, 23, doi: 10.1051/aas:2000169

Peña Ramírez, K., Béjar, V. J. S., Zapatero Osorio, M. R., Petr-Gotzens, M. G., & Martín, E. L. 2012, ApJ, 754, 30, doi: 10.1088/0004-637X/754/1/30

Peña Ramírez, K., Béjar, V. J. S., Zapatero Osorio, M. R., Petr-Gotzens, M. G., & Martín, E. L. 2012, ApJ, 754, 30, doi: 10.1088/0004-637X/754/1/30

Perez, F., & Granger, B. E. 2007, Computing in Science and Engineering, 9, 21, doi: 10.1109/MCSE.2007.53

Petr-Gotzens, M., Alcalá, J. M., Briceño, C., et al. 2011, The Messenger, 145, 29

Phillips, M. W., Tremblin, P., Baraffe, I., et al. 2020, A&A, 637, A38, doi: 10.1051/0004-6361/201937381

Rodrigo, C., & Solano, E. 2020, in XIV.0 Scientific Meeting (virtual) of the Spanish Astronomical Society, 182

Rodrigo, C., Solano, E., & Bayo, A. 2012, SVO Filter Profile Service Version 1.0,, IVOA Working Draft 15 October 2012 doi: 10.5479/ADS/bib/2012ivoa.rept.1015R

Rottensteiner, A., Petr-Gotzens, M. G., Meingast, S., et al. 2026, A&A, 706, A210, doi: 10.1051/0004-6361/202557533

Spiegel, D. S., Burrows, A., & Milsom, J. A. 2011, ApJ, 727, 57, doi: 10.1088/0004-637X/727/1/57

Taylor, M. B. 2005, in Astronomical Society of the Pacific Conference Series, Vol. 347, Astronomical Data Analysis Software and Systems XIV, ed. P. Shopbell, M. Britton, & R. Ebert, 29

Žerjal, M., Dominguez-Tagle, C., Vitas, N., et al. 2025, arXiv e-prints, arXiv:2503.22497, doi: 10.48550/arXiv.2503.22497

Wenger, M., Ochsenbein, F., Egret, D., et al. 2000, A&AS, 143, 9, doi: 10.1051/aas:2000332

Werner, M. W., Roellig, T. L., Low, F. J., et al. 2004, ApJS, 154, 1, doi: 10.1086/422992